MEDIUM-SCALE GRAVITY WAVE OBSERVATIONS USING AIRGLOW KEOGRAMS OVER THE BRAZILIAN COMANDANTE FERRAZ ANTARCTIC STATION

G. A. GIONGO [1]; C. M. WRASSE [1]; J. V. BAGESTON [2]; P. K. NYASSOR [1]; C. A. O. B. FIGUEIREDO [1]; P-D. PAUTET [3]; A. BILIBIO [1]; D. GOBBI [1]; H. TAKAHASHI [1].

[1] Space weather division, National Institute for Space Research; [2] Southern Space Coordination, National Institute for Space Research; [3] Center for Atmospheric and Space Sciences, Physics Department, Utah State University, USA.

Contact: gabriel.giongo@inpe.br

Introduction

Atmospheric gravity waves can propagate both vertically and horizontally through the atmosphere. These waves transport energy and momentum, known as wave stress, which connects different atmospheric layers and can lead to the atmosphere having a temperature different from the radiative equilibrium [1]. When these waves propagate vertically, they transport energy on a larger scale than other phenomena, influencing a significant portion of the middle and high atmosphere dynamics [2,3]. Despite numerous observations of gravity waves over the Antarctic Peninsula and the Drake Passage, which have revealed some characteristics of the waves and provided parameterizations of their activity in the stratosphere and mesosphere, there is still much to be investigated in terms of the wave spectra due to limitations in instruments and data processing. This study focuses on examining the characteristics of medium-scale gravity waves (MSGW) observed during the 2022 winter over the Antarctic Peninsula using keograms of all-sky airglow images expanding the general observation spectrum of the waves. Additionally, the study investigates the propagation behavior of the waves using a ray-tracing model.

Instrumentation and Methodology

The main instrument used to observe the gravity waves was an all-sky airglow imager installed at the Comandante Ferraz Antarctic Station (EACF), about 200 km from the tip of the Antarctic Peninsula (Figure 1). The instrument generates images of the OH emission layer, near 87 km of altitude (~6 km thickness), revealing the structures of the gravity waves propagating throughout the OH layer.

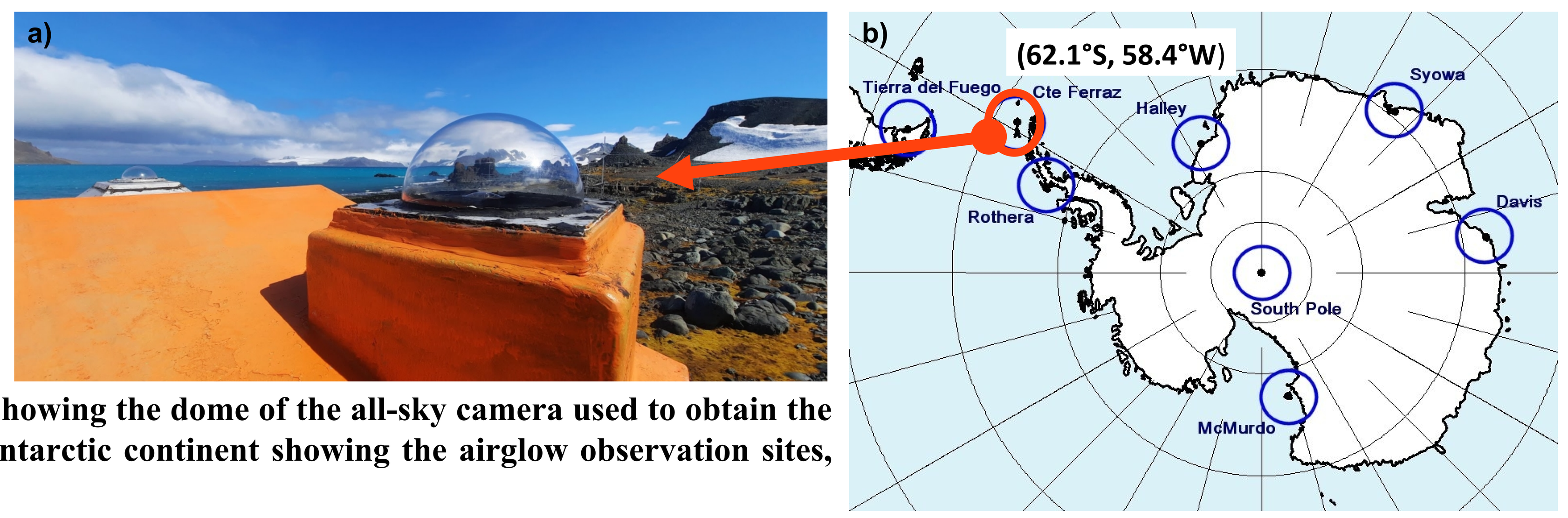

Figure 1: a) Punta Plaza facility showing the dome of the all-sky camera used to obtain the airglow images. b) Map of the Antarctic continent showing the airglow observation sites, with the EACF highlighted.

To identify more clearly the medium-scale gravity wave structures, keograms are made by sampling a row and a column of pixels at the image center and organizing these samples as a function of time. Oscillations with large horizontal wavelengths and long periods can be characterized by this technique. Keograms are filtered to remove low-period noises, like shown in Figure 2.

The analysis of the keograms is based on the wavelet method. First, a simple wavelet is applied to the time series of zenith pixels (the only series equivalent for both components of the keogram). The resulting wavelet spectrum is used to identify the main oscillation periods detected on the keogram. Figure 3 shows the wavelet spectra for the zenith time series of the keogram from Figure 2. The keograms are reconstructed based on the wavelet peak periods [4]. Figure 4 shows the reconstructed keograms for one of the main periods (79 min) identified in the wavelet analysis.

Phase lines of the reconstruction are used to estimate the phase difference (Δψ) between wave structures in order to calculate the wave parameters with the equations below. Figure 5 shows the phase lines at the time around the peak of the wavelet. The method was tested with synthetic waves simulations and the GW parameters calculated are in good agreement with simulated ones.

$$\lambda_{NS,EW} = \frac{\Delta d}{\Delta\psi/_{360°}}$$

$$\lambda_H = \frac{\lambda_{NS}\lambda_{EW}}{\sqrt{\lambda_{NS}^2 + \lambda_{EW}^2}}$$

$$C_H = \frac{\lambda_H}{\tau}$$

$$\phi = \cos^{-1}\left(\frac{\lambda_H}{\lambda_{NS}}\right)$$

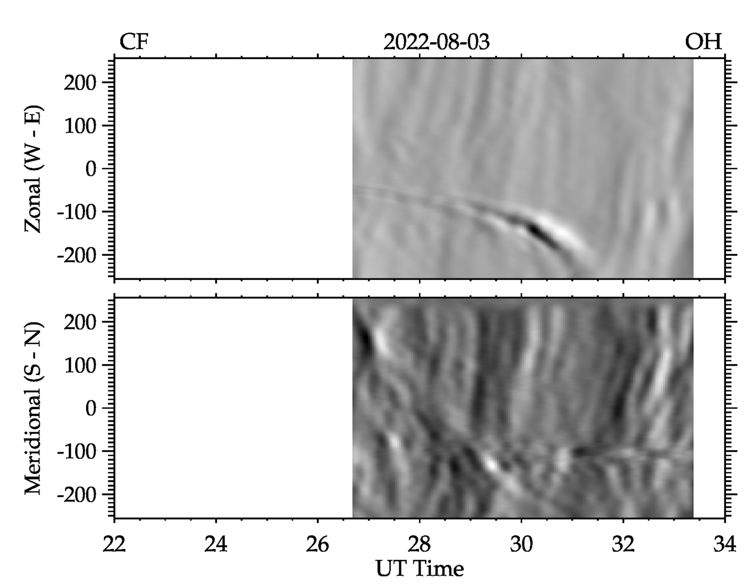

Figure 2: Filtered keogram for the night of August 3rd, 2022.

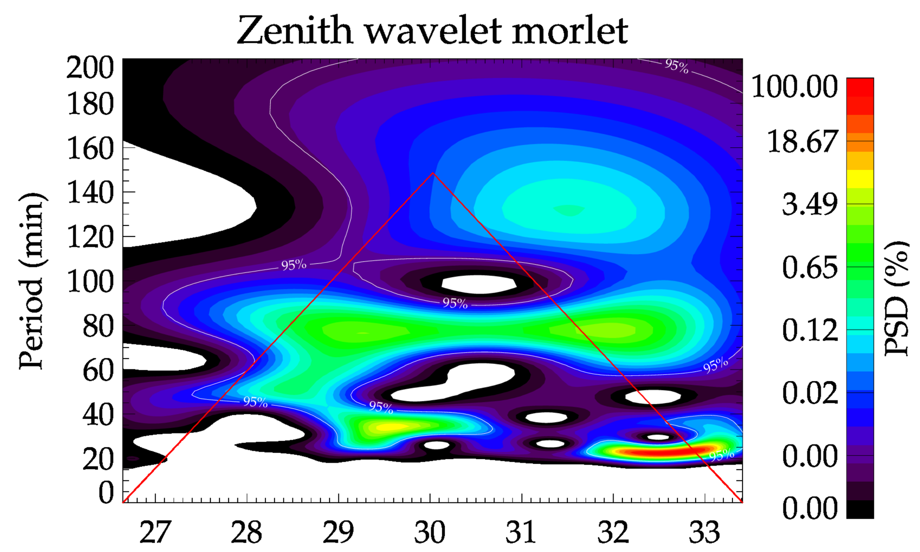

Figure 3: Wavelet spectrum for the zenith pixel of the image sequence.

Resulted parameters for wave in Figure 4.

λ (km)	529
τ (min)	79
C_h (m/s)	111
ϕ (°)	44

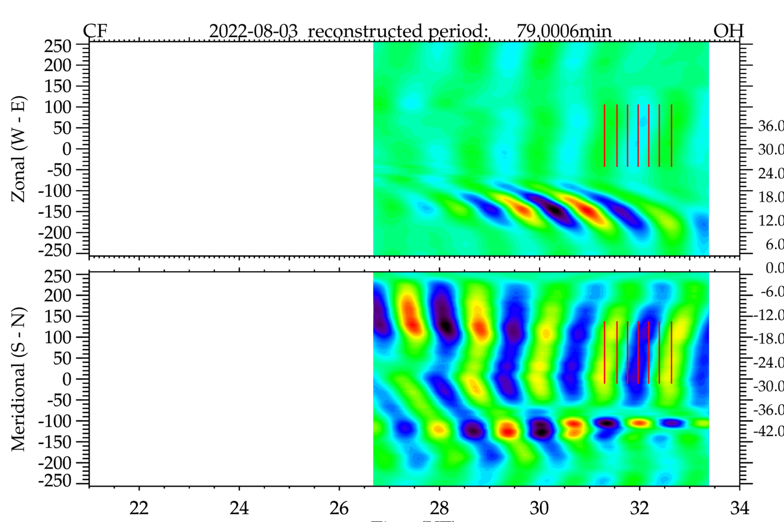

Figure 4: Reconstructed keogram for peak period 79 min.

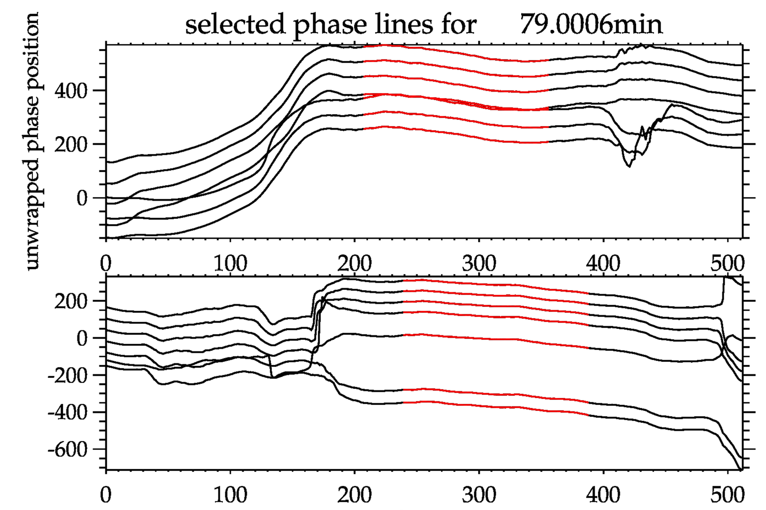

Figure 5: Phase lines of the reconstructed keogram. The red-highlighted region is the region where the linear fit is better.

Results

Figure 6 (a-c) shows the distribution of the observed gravity wave parameters retrieved by the spectral analysis. A total of 65 waves were analyzed, they presented horizontal wavelengths from 100 to 450 km, periods between 20 and 90 min, and phase speeds between 50 and 200 m/s.

Using wind data from a nearby meteor radar and SABER temperature soundings, when available in close proximity, intrinsic parameters, and vertical propagation characteristics were further estimated, and the histograms are shown in Figure 6 (d-g). The values of the estimated vertical wavelengths are distributed uniformly between 10 and 60 km, and the intrinsic parameters were found to be similar to those of the observed parameters. This quasi-similarity is due to the fast phase speed of the observed waves, which is much larger than the typical background wind speed at the observation altitude (about 88 km). With a few exceptions, the waves presented a majority of momentum fluxes below 10 m²/s²; even though their horizontal structure is larger, their amplitudes are small, and consequently, their influence in the atmosphere are also smaller.

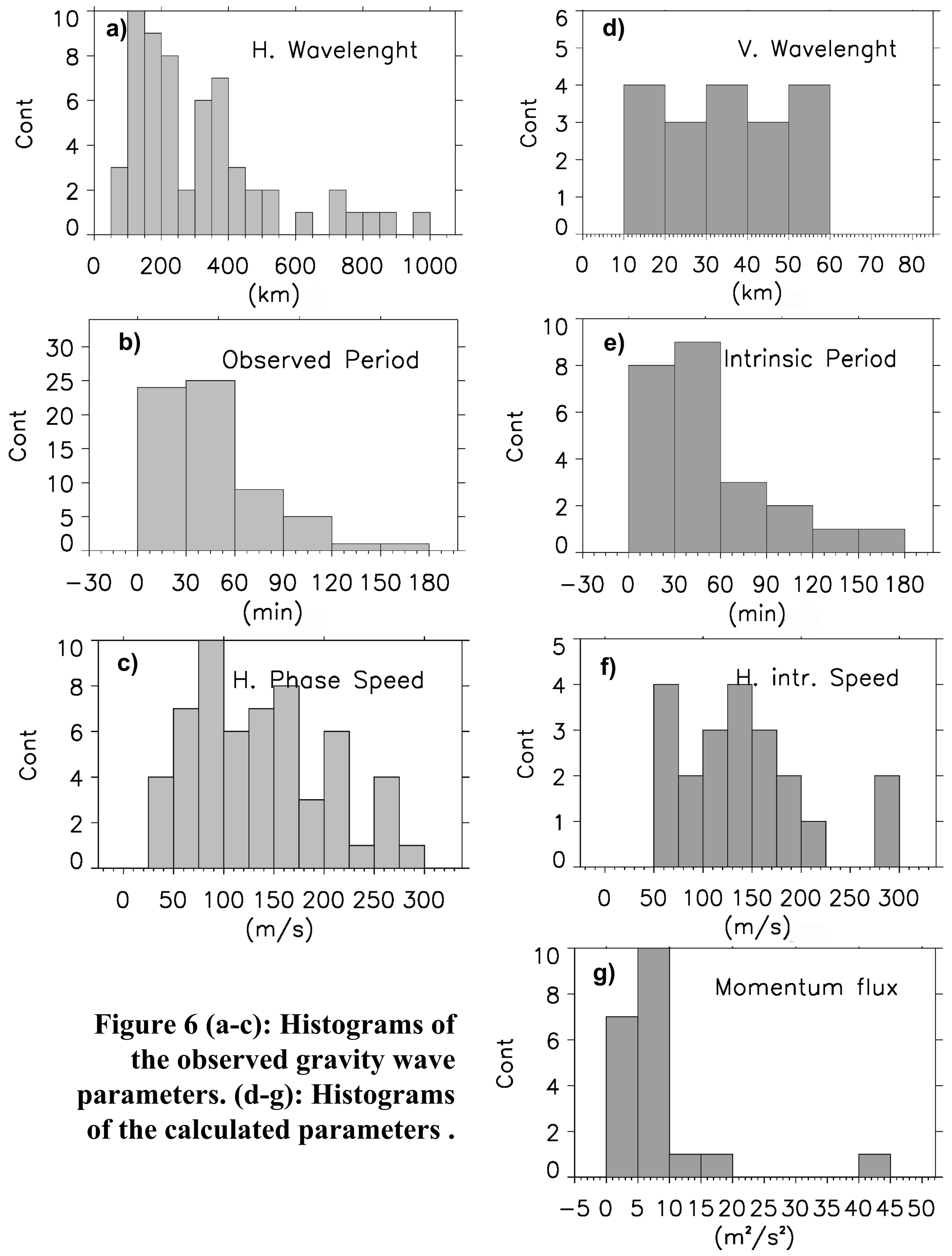

Figure 6 (a-c): Histograms of the observed gravity wave parameters. (d-g): Histograms of the calculated parameters .

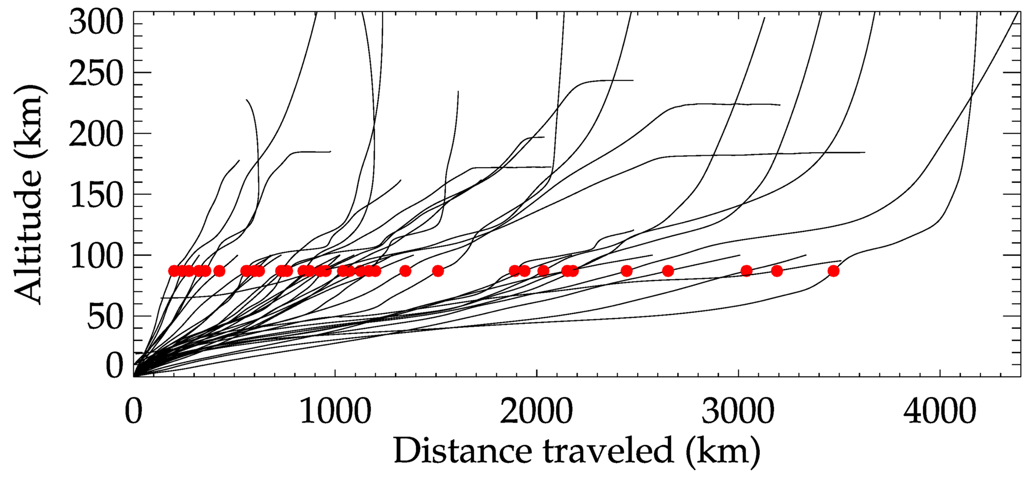

Figure 7: Diagram showing the traveled distance of the ray traced waves in function of the altitude. The red dots denote the observation altitude.

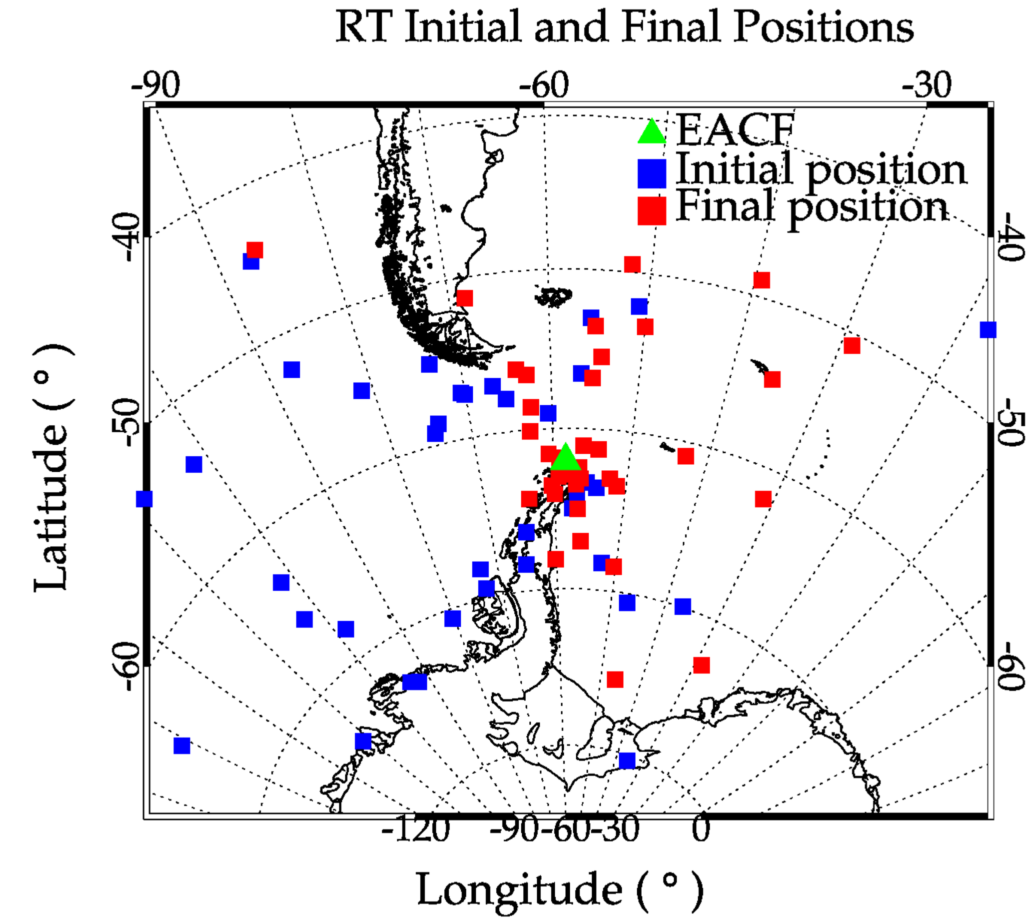

Figure 8: Initial and final positions of the ray-traced identified waves. Initial positions are estimated by backward ray-tracing, and final positions by forward ray-tracing.

The spectral analysis method was used to identify waves, and their paths were traced in both backward and forward directions to determine their sources in the lower atmosphere, and analyze their propagation behavior. The model takes into account anelastic dispersion relation with dissipation by viscosity and thermal diffusion [5].

In Figure 7, the distance traveled is plotted against the altitude of the ray-paths. It shows that a significant number of waves traveled longer distances through the stratosphere, where intense eastward winds, known as the polar vortex, prevail during winter. Above the observation altitude, the waves accelerate upward, with some of them propagating only horizontally above 180 km altitude. Many waves can propagate for very long distances mainly due to their large horizontal phase speeds.

Figure 8 shows the initial and final positions of the ray paths on a map of the surroundings of EACF. The propagation of the backward ray-paths is more dispersed at further distances from the station, while the forward ray-paths stopped at closer distances. This is consistent with the hypothesis that the waves are being horizontally advected by the stratospheric winds of the polar vortex.

Conclusions

Utilizing the keogram technique and a new spectral analysis methodology, parameters of 65 medium-scale gravity waves observed in 2022 over the Brazilian Antarctic Station Comandante Ferraz were estimated. Characteristics of the waves agree with the previous methodologies for other observation sites and represent a promising advance for expanding the airglow observation spectra over the Antarctic continent.

Preliminary results of the ray-tracing shows strong interaction of the waves with the stratospheric winds resulting in advection along the polar vortex direction.

Acknowledgments

The authors thank the NSF/CEDAR for the opportunity to participate, the CNPq by grant 140401/2021-0, CAPES (financial code 001) and FAPESP under grant 2019/05455-2.

References

[1] Fritts , D.C. e Alexander, M.J. Gravity wave dynamics and effects in the Middle atmosphere. Reviews of Geophysics, v. 41, n. 1, p. 3–1–3–64, 2003.

[2] C. Nappo, An Introduction to Atmospheric Gravity Waves, International Geophysics, Elsevier Science, 2002.

[3] J. R. Holton, An introduction to Dynamic Meteorology, Academic Press, 2004.

[4] Reichert et al. "Retrieval of Intrinsic Mesospheric Gravity Wave Parameters Using Lidar and Airglow Temperature and Meteor Radar Wind Data". Atmospheric Measurement Techniques, n 11, 2019.

[5] Vadas, S. L. Horizontal and vertical propagation and dissipation of gravity waves in the thermosphere from lower atmospheric and thermospheric sources. Journal of Geophysical Research: Space Physics, v. 112, n. A6, 2007.